Differential Transformation Based Adaptive Switching Control of Wind Turbines

Yang Liu[1], Yichen Zhang[2], Kai Sun[1], Xiaopeng Zhao[1]
[1]University of Tennessee, Knoxville, TN, USA (yliu161@vols.utk.edu, kaisun@utk.edu, xzhao9@utk.edu)
[2]Argonne National Laboratory, Lemont, IL, USA (e-mail: yichen.zhang@anl.gov)

***Abstract*—With the increasing penetration of wind generation and retirement of conventional coal-fired power plants, system frequency response may become inadequate under disturbances. Wind turbine generators can be switched to a frequency support mode once frequency deviation exceeds a preset deadband, not adapt to the disturbance. This paper proposes a new control strategy for wind turbine generators to adaptively switch between the normal operation mode and frequency support mode. The idea is to predict the safety of a frequency response in real time using a differential transformation method and activate a frequency support mode only when necessary. This control strategy effectively avoids unnecessary switches with the conventional deadband method but still ensure adequate frequency responses to disturbances.**

***Index Terms*— Frequency control, frequency response, wind turbine, switching control, differential transformation.**

I. INTRODUCTION

Wind power is playing an important role in achieve low carbonization [1]. However, the increasing penetration of wind power generation also poses great challenges to power system frequency responses [2]. One of the biggest challenges is the deteriorated system inertia response since the variable speed wind turbine generators (WTGs) are decoupled by power electronic interfaces from the main grid and cannot provide frequency support automatically [3]. Enabling WTGs to provide frequency support other than its normal operating mode is regarded as an effective way to improve frequency responses of high-renewable power grids.

Existing literature focused on designing controllers with WTGs for providing frequency support such as inertia emulation, primary frequency response, temporal power injection. Proposed control strategies can be categorized into two types: for the first type, a WTG normally works at the maximum power point tracking (MPPT) mode and can provide a temporary frequency support by releasing the kinetic energy stored in its rotor [4]-[5]; for the second type, a WTG works at a de-loaded condition and can provide a continuous frequency support by the reserved power output capability [6]-[7].

However, a critical issue faced by power system operators is to determine whether WTGs need to be switched to a frequency support mode under a disturbance. Therefore, some recent studies also focus on the timing of control mode switching, or equivalently, the setting of a deadband of frequency deviation to ensure adequate frequency response or enabling synthetic inertias for better frequency responses [8]-[10],[6]. The basic idea is to activate the frequency support mode only when frequency deviation exceeds a preset deadband. The proper choice of the deadband should make a WTG provide adequate frequency response while avoiding unnecessary switches for the purpose of wind farm revenue. GE has some recommended values for deadbands, e.g. 0.10 Hz for inertia response and 0.24 Hz for primary frequency response [8],[10]. However, these deadbands are often over conservative. Ref [8] aims at finding a critical deadband by identification of an approximate region of safety but its algorithm needs to solve a semi-definite programming problem by many iterations. How to switch the control mode of WTGs adaptively and effectively has not been solved.

To address this issue, this paper proposes a novel switching control strategy which predicts the safety of a frequency response right after a disturbance by evaluating the derived semi-analytical solutions of system frequency response model over a certain post-disturbance period of interest, and activates frequency support mode only when the frequency response is predicted as unsafe. The rationale of the proposed strategy is real time evaluation of an offline obtained semi-analytical solution on frequency responses using real-time measurements. Such a semi-analytical solution is in form of ultra-high order Taylor series derived by a differential transformation method (DTM) on the differential equation model of the system. The ultra-high order nature of the solution enables its largely extended convergence region to cover the frequency response period of interest, so that the frequency response of a WTG can be accurately predicted when a disturbance is detected and the WTG provides frequency support only for an unsafe response, thus avoiding the unnecessary switches. The case studies on a 4-bus power system and a New England 10-machine 39-bus system show the effectiveness of the proposed strategy.

In the rest of the paper, Section II is the problem description. Section III and IV present the proposed control strategy and the case study. Conclusions are in section V.

* This work was supported by the ERC Program of the U.S. NSF and DOE under grant EEC-1041877.

2022 IEEE Power & Energy Society General Meeting (PESGM) | 978-1-6654-0823-3/22/$31.00 ©2022 IEEE | DOI: 10.1109/PESGM48719.2022.9916811

II. PROBLEM DESCRIPTION

The system frequency response can be assessed using three metrics: the rate of change of frequency (ROCOF), frequency nadir and primary settling frequency. The effect of increasing wind power penetration on system frequency response can be illustrated in Figure. 1, where a larger ROCOF, lower frequency nadir and lower primary setting frequency are observed.

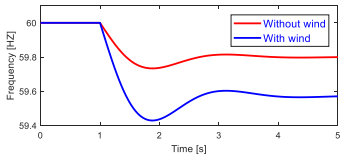

Figure 1. System frequency response with and without wind power

To address the inadequate frequency response issue, the WTGs are also expected to operate at frequency support mode in addition to its normal mode. Despite the many frequency support functions proposed in the literature, the strategies on switching among these modes are not carefully studied. A conceptual system frequency response where WTGs do not provide frequency support is shown in Fig. 2 with the case details and actual/ideal WTG reaction shown in Table I.

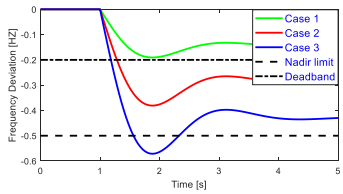

Figure 2. Frequency response under various disturbances

TABLE I. OPERATION STATUS OF FREQUENCY SUPPORT MODE

Situations	Disturbance	Actual status of frequency support	Ideal status of frequency support
Case 1	Small	Deactivated	Deactivated
Case 2	Medium	**Activated**	**Deactivated**
Case 3	Large	Activated	Activated

The WTG should activate its frequency support mode only for case 3 where the frequency deviation will otherwise surpass the nadir limit, and not react to the frequency deviations in case 1 and case 2. However, when the frequency surpasses the deadband but does not hit the nadir limit as in case 2, the frequency support will also be activated due to the deadband setting. The case 2 may occur frequently in WTG operations since the deadband setting is usually conservative to have some safety margin. These unnecessary frequency supports reduce the profits of wind farms and should be avoided. A straightforward way to reduce unnecessary switches is to set a larger deadband. However, a larger deadband can pose the system under higher risks of frequency excursions. Moreover, it is very hard to determine the critical deadband value with ensured safety. Therefore, the purpose of this paper is to investigate new methods to avoid unnecessary switches meanwhile ensuring adequate frequency responses.

III. PROPOSED ADAPTIVE SWITCHING CONTROL STRATEGY

Existing switching control strategies of WTGs fall into two categories, as shown in (1) and (2), respectively, where $\Delta w(t_0)$ is the frequency drop measured at $t=t_0$, Δw_{db} is a preset deadband width on the frequency deviation, $\Delta w_{crt}(\Delta p_d)$ is the critical deadband width, and Δp_d is a power imbalance assumed to be known under a disturbance.

$$\begin{aligned} &\text{if } \Delta w(t_0) < \Delta w_{db} : \text{in MPPT mode,} \\ &\text{otherwise: in frequency support mode} \end{aligned} \tag{1}$$

$$\begin{aligned} &\text{if } \Delta w(t_0) < \Delta w_{crt}(\Delta p_d) : \text{in MPPT mode,} \\ &\text{otherwise: in frequency support mode} \end{aligned} \tag{2}$$

The strategy in (1) is widely adopted by WTGs manufacturers due to its ease of implementation, e.g., the deadband width recommended by GE is Δw_{db}=0.15HZ for a certain frequency support mode [8],[10]. However, this strategy is not flexible to adapt to disturbances and the deadband width is often conservatively small such that the unnecessary mode switching of a WTG could be triggered. In comparison, the strategy in (2) can overcome the conservativeness, but it has to calculate a critical deadband width for each disturbance (e.g., by extensive simulation or by solving an optimization problem [8]), which is a huge computation burden and makes it difficult for real-time implementation.

A. Proposed Switching Control Strategy

To overcome the conservativeness and the computation burden of existing strategies (1) and (2), this letter proposes a novel switching control strategy in (3), where $\Delta w(t)$, $t\in[t_0,T]$ is the frequency response predictor and Δw_{lim} is the safety limit of frequency drop. The detailed derivation of the frequency response predictor is in Section II-C. It is observed from (3) that the proposed strategy uses frequency deviation at $t=t_0$, the time of detecting power imbalance such as loss of generation or load, but further predicts the frequency response over a future time period $(t_0,T]$. Also, the proposed strategy does not need a deadband since it directly compares the predicted frequency response with the safety limit.

$$\begin{aligned} &\textit{if } \Delta w(t) < \Delta w_{\lim} \text{ for } \forall t \in [t_0, T] : \text{in MPPT mode,} \\ &\text{otherwise: in frequency support mode} \end{aligned} \tag{3}$$

B. System Model

Consider the augmented frequency response model [8]-[9] in (4)-(5), where (4) is the classical frequency response model based on center of inertia, and (5) is the WTG model.

$$\begin{aligned} \Delta\dot{\omega} &= \frac{\omega_s}{2H}\left(\Delta p_m - \Delta p_d + \sum_{i=1}^{N}\Delta p_{gen,i} - \frac{D}{\omega_s}\Delta\omega\right) \\ \Delta\dot{p}_m &= \frac{1}{\tau_{ch}}\left(\Delta p_v - \Delta p_m\right) \\ \Delta\dot{p}_v &= \frac{1}{\tau_g}\left(-\Delta p_v - \frac{1}{R}\Delta\omega\right) \end{aligned} \tag{4}$$

$$\begin{aligned} \Delta\dot{\omega}_{r,i} &= A_i\Delta\omega_{r,i} + B_{1,i}\Delta\dot{\omega} + B_{2,i}\Delta\omega \\ \Delta p_{gen,i} &= C_i\Delta\omega_{r,i} + D_{1,i}\Delta\dot{\omega} + D_{2,i}\Delta\omega \end{aligned} \tag{5}$$

In (4), Δp_m, Δp_v are output power of turbines and governors; τ_{ch}, τ_g are their time constants, respectively; D and R are damping and droop coefficients; ω_s is the nominal frequency;

978-1-6654-0823-3/22/$31.00 ©2022 IEEE

N is the number of WTGs and i is the index of WTGs. In (5), $\Delta w_{r,i}$ and $\Delta p_{gen,i}$ are the rotor speed deviation and the increased power generation. Coefficients A_i and C_i are parameters of the WTG model; $B_{1,i}$ and $D_{1,i}$ are parameters for inertia emulation control mode; $B_{2,i}$ and $D_{2,i}$ are parameters for primary frequency control mode. Parameters $B_{1,i}$, $D_{1,i}$, $B_{2,i}$ and $D_{2,i}$ are zero for the MPPT mode and non-zero for frequency support modes.

C. Frequency Response Predictor

Given system state variables $\mathbf{x}$=[Δw, Δp_m, Δp_v, $\Delta w_{r,1}$,…, $\Delta w_{r,N}$]$^{\mathrm{T}}$ and the disturbance at time instant $t = t_0$, this section aims at finding a function $F(\mathbf{x}(t_0))$ in (6) to predict the frequency response over a future time period $(t_0,T]$.

$$\mathbf{x}(t_0 + \Delta t) = F(\mathbf{x}(t_0)), \forall \Delta t \in [0, T - t_0] \tag{6}$$

Since the analytical expression of (6) is generally unavailable, this letter seeks a semi-analytical, approximate solution about the frequency response in the form of power series of time in (7), where $f_k(\mathbf{x}(t_0))$ is the k^{th} order power series coefficients to be solved.

$$\mathbf{x}(t_0 + \Delta t) = \mathbf{x}(t_0) + f_1(\mathbf{x}(t_0))\Delta t + \cdots f_K(\mathbf{x}(t_0))\Delta t^K \tag{7}$$

To effectively solve the power series coefficients $f_k(\mathbf{x}(t_0))$, the DTM is adopted due to its proved accuracy and efficiency for solving detailed power system models in [11]-[13]. It provides various rules such as those in Table 2 to transform a function $x(t)$ directly to its power series coefficients $x[k]$.

TABLE II. SELECTED TRANSFORMATION RULES OF DTM

No.	Original functions	k^{th} order power series coefficients
1	$ax(t) + b$	$aX[k] + b\delta[k]$, where $\delta[0] = 1; \delta[k] = 0, k \geq 1$
2	$x^2(t)$	$\sum_{m=0}^{k} X[m]X[k-m]$
3	$\dot{x}(t)$	$(k+1)X[k+1]$
⋮	⋮	⋮

By applying these rules to each term in (4)-(5), a recursive equation about the k^{th} order power series coefficients $f_k(\mathbf{x}(t_0))$=[$\Delta w[k]$, $\Delta p_m[k]$, $\Delta p_v[k]$, $\Delta w_{r,1}[k]$,…, $\Delta w_{r,N}[k]$]$^{\mathrm{T}}$ is obtained in (8)-(12).

$$\begin{aligned}(k+1)\Delta w[k+1] = \frac{\omega_s}{2H}(&\Delta p_m[k] - \Delta p_d\delta[k] \\ &+\textstyle\sum_{i=1}^{N}\Delta p_{gen,i}[k] - \frac{D}{\omega_s}\Delta w[k])\end{aligned} \tag{8}$$

$$(k+1)\Delta p_m[k+1] = \frac{1}{\tau_{ch}}\ \Delta p_v[k] - \Delta p_m[k] \tag{9}$$

$$(k+1)\Delta p_v[k+1] = \frac{1}{\tau_g}\left(-\Delta p_v[k] - \frac{1}{R}\Delta w[k]\right) \tag{10}$$

$$\begin{aligned}(k+1)\Delta w_{r,i}[k+1] = A_i\Delta w_{r,i}[k] + B_{2,i}\Delta w[k] \\ +B_{1,i}\cdot(k+1)\Delta w[k+1]\end{aligned} \tag{11}$$

$$\begin{aligned}\Delta p_{gen,i}[k] = C_i\Delta w_{r,i}[k] + D_{2,i}\Delta w[k] \\ +D_{1,i}\cdot(k+1)\Delta w[k+1]\end{aligned} \tag{12}$$

The derivation of (8) is elaborated below as an example. The remaining equations (9)-(12) are obtained similarly:

First, the left-hand side of (8) is obtained using the rule 3:

$$\Delta\dot{\omega} \rightarrow (k+1)\Delta w[k+1]$$

Second, the right-hand side of (8) is obtained using rule 1:

$$\Delta p_m - \Delta p_d \rightarrow \Delta p_m[k] - \Delta p_d\delta[k]$$

$$\textstyle\sum_{i=1}^{N}\Delta p_{gen,i} \rightarrow \sum_{i=1}^{N}\Delta p_{gen,i}[k]$$

$$-\frac{D}{\omega_s}\Delta\omega \rightarrow -\frac{D}{\omega_s}\Delta w[k]$$

$$\frac{\omega_s}{2H}\left(\Delta p_m - \Delta p_d + \textstyle\sum_{i=1}^{N}\Delta p_{gen,i} - \frac{D}{\omega_s}\Delta\omega\right) \rightarrow$$

$$\frac{\omega_s}{2H}(\Delta p_m[k] - \Delta p_d\delta[k] + \textstyle\sum_{i=1}^{N}\Delta p_{gen,i}[k] - \frac{D}{\omega_s}\Delta w[k])$$

Finally, (8) is obtained by equating both sides.

With the derived recursive equations (8)-(12), the power series coefficients $f_k(\mathbf{x}(t_0))$ up to any desired order can be derived. Especially, the frequency response at time instant t=t_0+Δt is predicted by power series of time in (13).

$$\Delta w(t_0 + \Delta t) = \Delta w[0] + \Delta w[1]\Delta t + \cdots \Delta w[K]\Delta t^K \tag{13}$$

The predicted frequency response (13) is accurate within a certain time period whose length increases with the order K. To ensure the accuracy of the predicted frequency response over a longer time period of interest, arbitrary high order K such as 100 to 200 can be easily derived by the DTM method. Besides, the multi-time window strategy [11] can be used to further enhance the accuracy of (13). For illustration, the first three terms in the right-hand side of (13) are derived below.

First, initialize $f_0(\mathbf{x}(t_0))$=[$\Delta w[0]$, $\Delta p_m[0]$, $\Delta p_v[0]$, $\Delta w_{r,1}[0]$,…, $\Delta w_{r,N}[0]$]$^{\mathrm{T}}$ = [$\Delta w(t_0)$, $\Delta p_m(t_0)$, $\Delta p_v(t_0)$, $\Delta w_{r,1}(t_0)$,…, $\Delta w_{r,N}(t_0)$]$^{\mathrm{T}}$. Second, $f_1(\mathbf{x}(t_0))$=[$\Delta w[1]$, $\Delta p_m[1]$, $\Delta p_v[1]$, $\Delta w_{r,1}[1]$,…, $\Delta w_{r,N}[1]$]$^{\mathrm{T}}$ is calculated by

$$\Delta w[1] = \frac{\omega_s}{2H}(\Delta p_m(t_0) - \Delta p_d + \textstyle\sum_{i=1}^{N}\Delta p_{gen,i}[0] - \frac{D}{\omega_s}\Delta w(t_0))$$

$$\Delta p_m[1] = \frac{1}{\tau_{ch}}\ \Delta p_v(t_0) - \Delta p_m(t_0)$$

$$\Delta p_v[1] = \frac{1}{\tau_g}\left(-\Delta p_v(t_0) - \frac{1}{R}\Delta w(t_0)\right)$$

$$\Delta w_{r,i}[1] = A_i\Delta w_{r,i}(t_0) + B_{2,i}\Delta w(t_0) + B_{1,i}\Delta w[1]$$

$$\Delta p_{gen,i}[0] = C_i\Delta w_{r,i}[0] + D_{2,i}\Delta w[0] + D_{1,i}\cdot\Delta w[1]$$

Then, $\Delta w[2]$ is calculated by

$$\Delta w[2] = \frac{\omega_s}{2H}(\Delta p_m[1] + \textstyle\sum_{i=1}^{N}\Delta p_{gen,i}[1] - \frac{D}{\omega_s}\Delta w[1])$$

Finally, $\Delta w(t_0 + \Delta t) = \Delta w[0] + \Delta w[1]\Delta t + \Delta w[2]\Delta t^2$.

978-1-6654-0823-3/22/$31.00 ©2022 IEEE

IV. CASE STUDY

A. Test on a 4-bus system

To validate the effectiveness of the proposed strategy, a four-bus system in [8] is used, shown in Fig. 3. The synchronous generator at bus 1 represents a 600 MW conventional generation, aggregated from four thermal power plants with 150 MW capacity each. The WTG at bus 3 represents a 300 MW wind power generation, aggregated from 200 DFIGs with 1.5 MW capacity each. The parameters in the frequency response model and the WTG model are adopted from [8] where A_i = -0.0723, C_i = 0.0127, H=4, τ_{ch} = 0.3, τ_g = 0.1, ω_s = 60HZ, D = 1, R = 0.05, $B_{1,i}$=-0.6246, $B_{2,i}$=0.1874, $D_{1,i}$=-0.10, $D_{2,i}$=-0.03, Δw_{db}=0.2 HZ and Δw_{lim}=0.5 HZ.

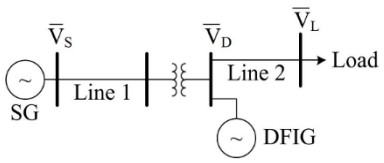

Figure 3. Diagram of four-bus test system

The accuracy of the proposed DTM-based semi-analytical solution is tested under three scenarios with different disturbance severities, shown in Table 3. The commonly used numerical integration method RK4 is used as the benchmark. The system frequency response over a time window of 4 seconds after the disturbance occurs is studied. In the RK4 method, a time step of 0.04 second is used and 100 consecutive time windows are used to make the frequency response solution. In the semi-analytical solution in (9), $K = 200$ is selected. The accuracy of the semi-analytical solution is shown in Fig. 4. Under all three scenarios, the semi-analytical solution matches the RK4 solution up to $t = 4.4$ s, i.e. equal to 340 consecutive time intervals of RK4. The effect of order K on the semi-analytical solution accuracy is also studied. The convergence region of the semi-analytical solution is drawn in Fig. 5. It shows the convergence region of the semi-analytical solution increases with its order. For the four-bus system, the frequency nadir limit usually happens before $t = 2$ s. Therefore, an order $K = 50$ is selected for the proposed control strategy.

To show the proposed adaptive switching strategy can check the safety in real time, the time cost of evaluating the analytical solution are compared with the time for frequency to reach the deadband in the worst-case scenario 3. In Fig. 4c), it takes 0.19 second for the frequency deviation to hit the deadband $\Delta\omega = 0.2$ Hz, while the time cost for evaluating the analytical solution (9) with $K = 50$ at one time instant is only 6.04×10^{-4} second. It means the analytical solution evaluation can be done at more than 300 time instants before the deadband is met. Moreover, evaluations of an analytical solution at different time instants are independent from each other and hence can be conducted by parallel computers. Therefore, the proposed control strategy has enough time to check the safety of a frequency response and bypass the deadband for a safe response to avoid unnecessary switches.

TABLE III. SETTINGS OF THE THREE SCENARIOS

Scenarios	Disturbance	Δp_d (MW)
Scenario 1	Small	50
Scenario 2	Medium	100
Scenario 3	Large	150

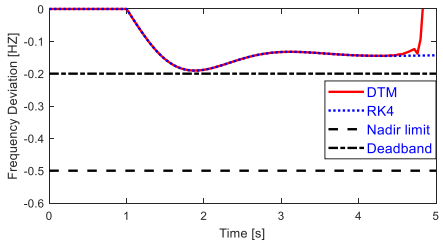

a) Scenario 1: small disturbance

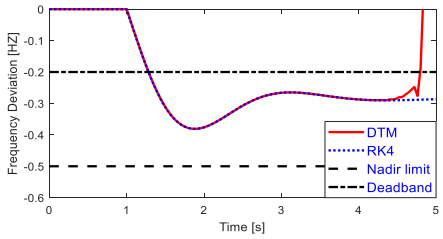

b) Scenario 2: medium disturbance

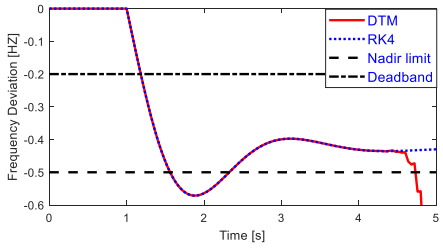

c) Scenario 3: large disturbance

Figure 4. Comparisons of DTM and RK4

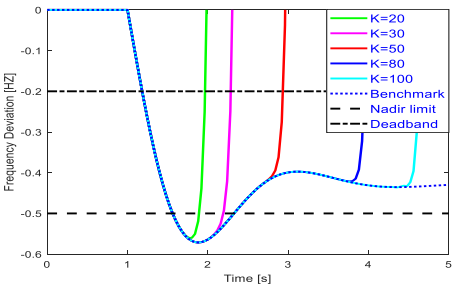

Figure 5. Frequency responses using DTM-based semi-analytical solutions with different orders

To validate the proposed control strategy in avoiding unnecessary switches, the disturbances Δp_d are changed from 10 MW to 150 MW with the step size of 10 MW shown in Fig. 6. Among the 15 cases, only 2 cases require WTGs to provide frequency support and they are successfully detected by the safety check in the proposed control strategy. Otherwise, the WTGs will be switched to frequency support modes in 10 cases, where 8 of them are switched unnecessarily.

978-1-6654-0823-3/22/$31.00 ©2022 IEEE

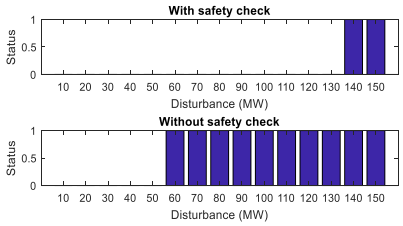

Figure 6. Switching of the frequency support mode with and without safety check(1 – switched; 0 – unswitched)

The proposed adaptive switching control strategy not only avoids the unnecessary switches, but also lets the WTGs react correctly when the switching is indeed needed. For the worst-case scenario 3, the proposed strategy successfully sensed the unsafety, and the frequency support mode is activated timely. The frequency response when switching to different frequency support modes at $\Delta\omega = 0.2$ Hz is shown in Fig. 7, where mode 1 is the MPPT mode and the other modes represent frequency control modes with different control parameters $B_{1,i}$, $B_{2,i}$, $D_{1,i}$, $D_{2,i}$. It shows the safety is preserved for all frequency support modes using the proposed strategy.

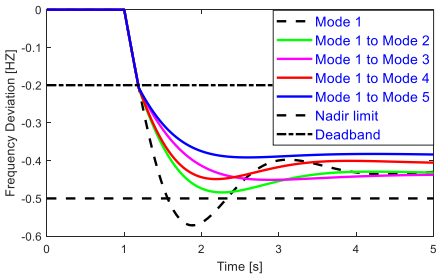

Figure 7. Frequency response when WTGs are switched to frequency support modes at $\Delta\omega = 0.2$ HZ

B. Test on the 39-bus system

To test the performance of the proposed strategy on real-world power system, a 10-machine 39-bus system is used where five synchronous generators are replaced by WTGs. The parameters in (4)-(5) are the same with the 4-bus system.

Two scenarios, i.e., a safe scenario with power imbalance of -500 MW and an unsafe scenario with power imbalance of -1000MW, are tested. Fig. 1 and Fig. 2 give the frequency responses in the two scenarios. The proposed strategy activates the frequency support mode only for the unsafe scenario. In contrast, the deadband based strategy would activate frequency support for both the safe and unsafe scenarios. This result shows the proposed strategy can overcome conservativeness compared with the deadband based strategy.

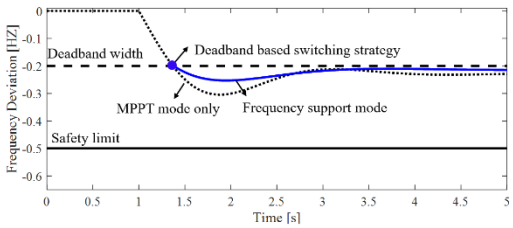

Figure 8. Switching strategy for the safe frequency response

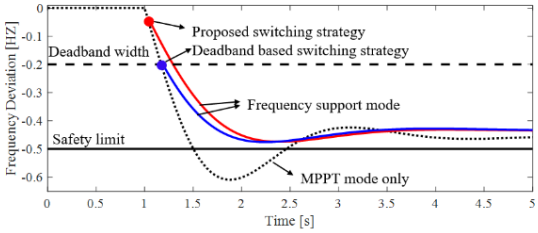

Figure 9. Switching strategy for the unsafe frequency response

V. CONCLUSIONS

This paper proposes an analytical, adaptive switching control strategy to overcome the conservativeness of the deadband based strategy. For safe responses, the frequency support mode is not activated even if the deadband is met. For unsafe responses, the frequency support mode is activated immediately once unsafety is predicted. The strategy is shown effective to control WTGs for adequate frequency response.

REFERENCES

[1] J. Dong, F. Gao, X. Guan, Q. Zhai, and J. Wu, "Matching a desirable generation pattern for large-scale wind farm with autonomous energy storage control strategy," in *Proc. 2015 IEEE Power & Energy Society General Meeting*, pp. 1-5.

[2] N. Nguyen and J. Mitra, "An analysis of the effects and dependency of wind power penetration on system frequency regulation," *IEEE Trans. Sustain. Energy*, vol. 7, no. 1, pp. 354–363, Jan. 2016.

[3] D. Gautam, L. Goel, R. Ayyanar, V. Vittal, and T. Harbour, "Control strategy to mitigate the impact of reduced inertia due to doubly fed induction generators on large power systems," *IEEE Trans. Power Syst.*, vol. 26, no. 1, pp. 214–224, Feb. 2011.

[4] J. Morren, S. W. H. de Haan, W. L. Kling, and J. A. Ferreira, "Wind turbines emulating inertia and supporting primary frequency control," *IEEE Trans. Power Syst.*, vol. 21, no. 1, pp. 433–434, Feb. 2006.

[5] B. Wang, Y. Zhang, K. Sun, K. Tomsovic, "Quantifying the synthetic inertia and load-damping effect of a converter-interfaced power source," in *Proc. 2018 IEEE International Energy Conference (ENERGYCON)*, pp. 1-6.

[6] S. Wang and K. Tomsovic, "A novel active power control framework for wind turbine generators to improve frequency response," *IEEE Trans. Power Syst.*, vol. 33, no. 6, pp. 6579-6589, Nov. 2018.

[7] R. G. de Almeida and J. A. Pecas Lopes, "Participation of doubly fed induction wind generators in system frequency regulation," *IEEE Trans. Power Syst*., vol. 22, no. 3, pp. 944–950, Aug. 2007.

[8] Y. Zhang, K. Tomsovic, S. M. Djouadi, and H. Pulgar-Painemal, "Hybrid controller for wind turbine generators to ensure adequate frequency response in power networks," *IEEE J. Emerg. Sel. Top. Circuits Syst*., vol. 7, no. 3, pp. 359–370, Sep. 2017.

[9] Y. Zhang, M. E. Raoufat, K. Tomsovic, and S. M. Djouadi, "Set theory-based safety supervisory control for wind turbines to ensure adequate frequency response," *IEEE Trans. Power Syst*., vol. 34, no. 1, pp. 680-692, Jan. 2019.

[10] K. Clark, N. W. Miller, and J. J. Sanchez-Gasca, "Modeling of GE wind turbine-generators for grid studies," General Elect. Int., Schenectady, NY, USA, Tech. Rep. Version 4.5, 2010.

[11] Y. Liu, K. Sun, R. Yao, B. Wang, "Power system time domain simulation using a differential transformation method," *IEEE Trans. Power Syst.*, vol. 34, no. 5, pp. 3739-3748, Sept. 2019.

[12] Y. Liu and K. Sun, "Solving power system differential algebraic equations using differential transformation," *IEEE Trans. Power Syst.*, vol. 35, no. 3, pp. 2289-2299, May 2020.

[13] Y. Liu, K. Sun, J. Dong, "A dynamized power flow method based on differential transformation," *IEEE Access*, vol. 8, pp. 182441-182450, 2020.

978-1-6654-0823-3/22/$31.00 ©2022 IEEE